A Technique for Stacking Digitized Photographic Plates

Abstract

With the advent of fast scanning microphotometers and inexpensive digital mass storage, there has been a resurgence of interest in performing deep ($B \leq 25$) panoramic surveys by co-adding large numbers ($\sim 10^2$) of digitized photographic plates. While the Kodak IIIa emulsions are highly linear recorders of photographic grain density, we demonstrate that the threshold and saturation levels which restrict the dynamic range of the emulsion can distort the higher statistical moments of the grain density fluctuations (variance, skewness, etc.) along the linear part of the characteristic curve. The variance of the grain fluctuations is only additive between digitized plates that preserve the Poissonian grain noise. In order to compensate for the statistical distortion, we derive the necessary pixel weighting for five scanning aperture sizes (2 μm, 4 μm, 8 μm, 16 μm, 32 μm) as a function of the grain density.

1. Introduction

Wide-field photographic plates continue to play a crucial rôle in astronomical surveys (West 1991; Irwin 1992). In an age of rapidly evolving electronic detectors, plates still retain the unique ability to record high-density photometric information over fields of view exceeding a few degrees with a spatial resolution limited only by the seeing. Recent improvements in the performance of fast scanning microphotometers (e.g. COSMOS) now make it possible to extract $\sim 10^9$ data pixels from a plate in a matter of a few hours. This has allowed various groups to compile objective catalogues of very large numbers of galaxies. In the Edinburgh/Durham Galaxy Survey, Heydon-Dumbleton et al. (1988) scanned 60 overlapping plates that cover almost one steradian of the southern sky in order to compile a catalogue of roughly one million galaxies down to a limiting magnitude of $B_J \approx 20$. Rapid plate scanning also affords the opportunity to co-add or 'stack' a large number of photographic plates in order to increase detection limit sensitivity over a wide field. Tsvetkov (1992) reports that there are at least 1.3 million wide-field plates in archives throughout the astronomical community. Roughly speaking, this means that each square degree is covered by $30\,f^2$ plates, where f is the average field size in degrees, although these archives are heavily biased towards certain regions of the sky largely in the northern hemisphere. Moreover, a fair proportion of the plate archives will have been taken under less than ideal conditions, and hence will be of little use.

Malin (1988) has demonstrated that the plate limit improves by about two magnitudes when 36 UK Schmidt plates are co-added using traditional laboratory techniques. More recently, Hawkins (1991) used the COSMOS microphotometer to scan 58 plates of a common field; these were added in density space to form an image whose completeness limit was $B_J \approx 24$ mag with some images going a magnitude fainter. The importance of this result is exemplified by the number-magnitude relation for field galaxies: an improvement in the limiting sensitivity from $B_J = 22$ mag to $B_J = 24$ mag increases the detection rate of field galaxies by an order of magnitude.

2. The Statistics of Photographic Plates

For a given aperture size, the central limit theorem ensures that the density fluctuations obey Poissonian or Gaussian statistics (Marriage & Pitts 1956), even in the limit that the scanning aperture size is of order the emulsion grain size (Trabka 1969). However, it is clear from Fig. 1a that the width of the grain noise statistics does not conform to a simple Poissonian ($\sqrt{N}$) model. This is underscored by Fig. 1b which shows that there is a systematic trend in the skewness of the density fluctuations with increasing grain density. In the following section, we present a statistical treatment that attempts to explain the basic behavior in Figs. 1a and 1b. Any departure from Poissonian statistics has important consequences for co-adding digitized photographic plates.

When we add together separate images with mean signal s_1 and s_2, it is normally assumed that the noise in both images, n_1 and n_2, obeys Poissonian statistics. If $n_1 = \epsilon_1\sqrt{s_1}$ and $n_2 = \epsilon_2\sqrt{s_2}$, the

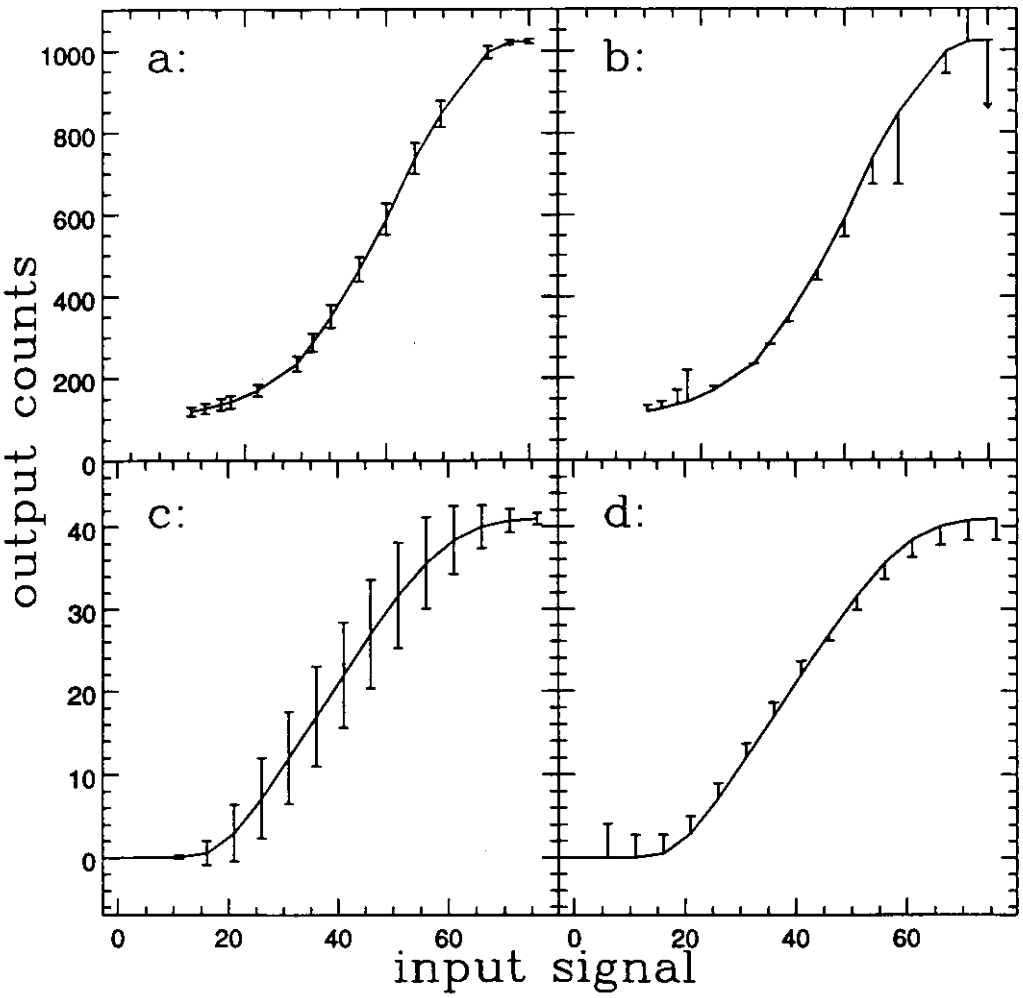

Figure 1. a, b. The characteristic curve (or μ) for a scanned IIIa-F photographic plate measured from the density step wedges. In **a**, the error bars correspond to $\pm 1\sigma$, and in **b**, the vertical bars indicate the magnitude and sign of the skewness, κ. **c, d.** The output response to a linear detector in the presence of saturation and threshold levels. When the linear response is restricted to a finite dynamic range, both moments deviate from their true Poissonian values.

variance of the noise in the summed image is simply the sum in quadrature of the original variances, i.e., $\sqrt{n_1^2+n_2^2}=\sqrt{\epsilon_1^2 s_1+\epsilon_2^2 s_2}$. Therefore, in summing images, we are making at least two general assumptions: n_1 and n_2 are statistically independent and are governed by Poissonian noise such that $\epsilon_1 = \epsilon_2 = 1$. The first assumption is discussed by Shopbell, Bland-Hawthorn & Malin (1992) and reduces to showing that the weight of the covariance term, w_3, is negligible, viz.

$$\sigma_S^2=w_1 n_1^2+w_2 n_2^2+w_3 n_1 n_2 \qquad (1)$$

where $w_1 = \epsilon_1^{-2}$, $w_2 = \epsilon_2^{-2}$, and σ_S^2 is the variance of the summed image. For the second assumption, if the noise distributions deviate from Poisson statistics, the correction factors w_1 and w_2 need to be applied to the individual variances. These weights are derived below.

3. The Restricted Poissonian Distribution

The photographic plate is a highly linear recorder of photographic density. After Dainty & Shaw (1974), we demonstrate that the measured density fluctuations in Figs. 1a and 1b can be understood with a relatively straightforward model. For ease of illustration, consider a linear *photon* detector comprising an infinite number of recording cells that is uniformly exposed with an average number of p photons per cell. The photon distribution over the cells will be governed by Poisson statistics such that the proportion of cells receiving r photons will be $p^r e^{-p}/r!$. In practice, there are minimum (threshold) and maximum (saturation) exposure levels that a detector can register. Assume that the first $(t - 1)$ photons do not generate counts whereas the tth photon registers one count. Assume further that s or a higher number of photons register exactly s counts. The mean number of counts over all cells is then

$$\mu = E(p) = \alpha(1 - \beta e^{-p}) \tag{2}$$

where $\alpha = s - t + 1$ and

$$\beta = \frac{1}{\alpha} \sum_{k=t-1}^{s-1} \sum_{r=0}^{k} \frac{p^r}{r!} \tag{3}$$

We have used the form of the expectation, E, to determine higher moments of the distribution, viz.

$$E(p^2) = \alpha^2(1 - \gamma e^{-p}) \tag{4}$$

$$E(p^3) = \alpha^3(1 - \delta e^{-p}) \tag{5}$$

where the summation terms are given by

$$\gamma = \frac{1}{\alpha^2} \sum_{k=t-1}^{s-1} \sum_{r=0}^{k} (2[k-t+2]-1)\frac{p^r}{r!} \tag{6}$$

$$\delta = \frac{1}{\alpha^3} \sum_{k=t-1}^{s-1} \sum_{r=0}^{k} (3[k-t+2][(k-t+2)-1]+1)\frac{p^r}{r!} \tag{7}$$

Equations (4) and (5) provide information on the variance, σ^2, and the skewness, κ, of the distribution, since

$$\sigma^2 = E(p^2) - \mu^2 \tag{8}$$

$$\kappa^3 = E(p^3) - 3\mu\sigma^2 - \mu^3 \tag{9}$$

For an ideal linear detector with infinite dynamic range, the expected values of the mean, standard deviation and skewness for a Poisson distribution are easily derived. In the presence of detector limits, all three statistical moments deviate from their true Poissonian values; the induced 'statistical distortion' is illustrated in Figs. 1c and 1d. Intuitively, as the value of p approaches either detector limit from the linear section of the curve, one tail of the distribution measuring the statistical uncertainty in p starts to disappear. A comparison of Figs. 1a and 1b with Figs. 1c and 1d respectively reveals that the restricted Poissonian model explains the major trends in the scanned density step wedges.

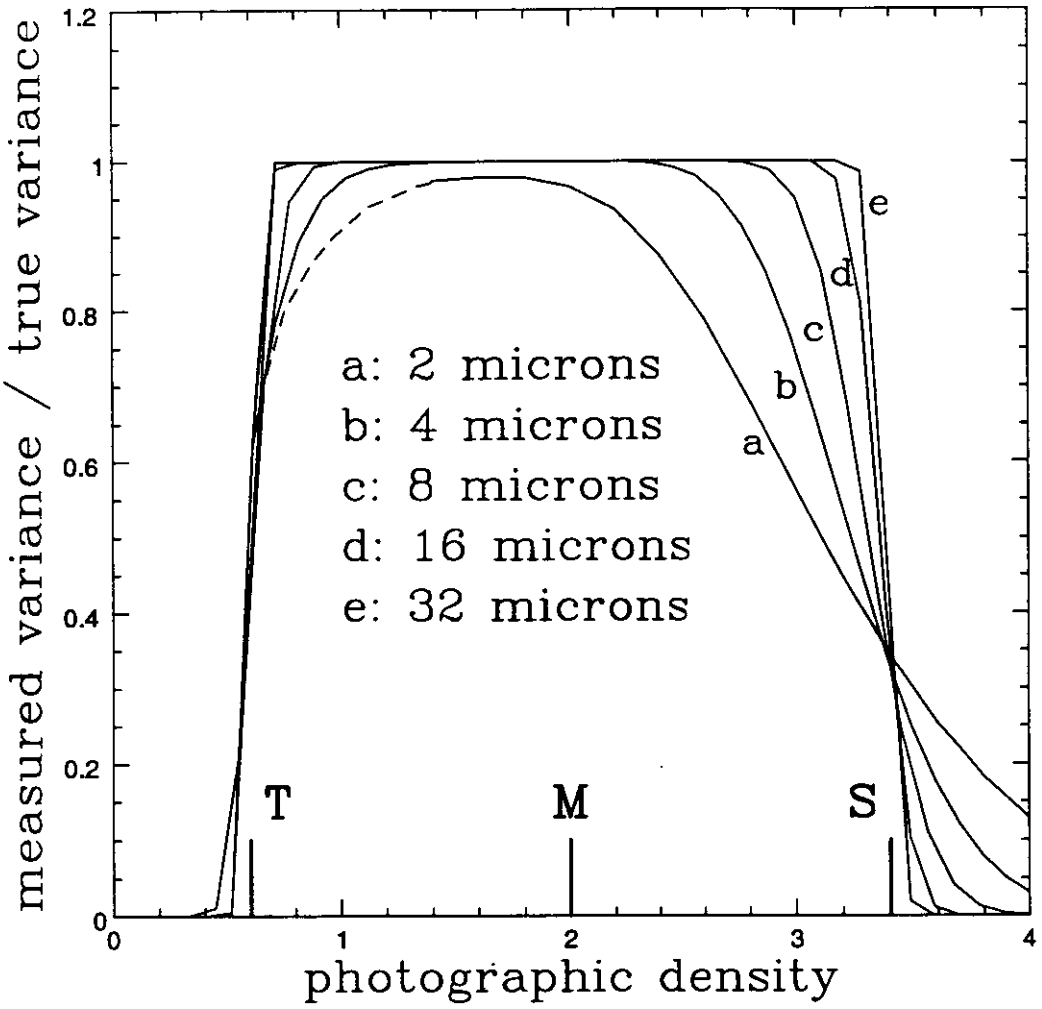

Figure 2. A plot that shows how the measured variance differs from the Poissonian variance as a function of photographic density and scanning aperture size. The values along the vertical axis are inversely related to the corrective weights (see text). The statistical distortion is clearly more important at high density and for small scanning apertures. The dashed line is an extrapolation as the numerical method fails in this region.

4. Discussion

In order to simulate the response of the grain density fluctuations to the presence of threshold and saturation levels, we determine the linear dynamic range that produces the fluctuation level at some intermediate (midpoint) value along the straight section of the characteristic curve. We note in Fig. 1 that the maximum statistical dispersion occurs roughly at the midpoint of the linear ramp. Since the threshold and saturation levels can only reduce the statistical dispersion, it follows that the grain density for which the statistical response is most likely to exhibit Poissonian behavior is that which produces the largest grain dispersion. Furenlid, Schoening & Carder (1977) have calibrated the grain density fluctuations, σ_D, on the linear part of the characteristic curve for a range of photographic emulsions. They find that under a wide range of conditions, there exists a unique relationship between σ_D and grain density, D: for the Kodak IIIa emulsions, we adopt $(\sigma_D/D) = (0.64/a)$ where a is the square aperture dimension in microns. We compute statistical models which attempt to simulate the grain density response for five aperture sizes; 2, 4, 8, 16, 32 μm. The expected grain density fluctuations are 32%, 16%, 8%, 4%, 2% respectively. For all five models, the positions of the threshold (T), midpoint (M) and saturation (S) levels remain in a fixed ratio with respect to the linear scale defined by a zero density (Z) and a peak density (P). We adopt the following representative density values in each of the simulations: Z = 0.0, T = 0.6, M = 2.0, S = 3.4, P = 4.0. An important boundary condition in our model is that the density fluctuation falls to zero at zero density. However,

in reality, we note from Fig. 1a that there will be finite background noise at both extremes of the density range. The results are summarized in Fig. 2. It is clear that the statistical distortion is particularly severe for the smaller apertures and tends to restrict the linear density response, particularly to higher densities. For a scanning aperture of 4 μm, notice that the higher statistical moments are truly Poissonian for only about half of the straight section of the characteristic curve.

In practice, one corrects for the statistical distortion by dividing out the form of the measured to true variance in Fig. 2. The necessary pixel weights, w_1 and w_2, are functions of density and are essentially the reciprocal of the values plotted in Fig. 2. The first statistical moment is handled by the density-to-intensity transformation; the third and higher moments are unlikely to have much influence. In stacking N digitized plates, with the proposed corrections, we would expect the magnitude limit to improve in proportion to 2.5 log $\sqrt{N}$. Thus, a hundred co-added plates could in principle increase the sensitivity limit by an order of magnitude everywhere within the full field.

References

Dainty, J.C. & Shaw, R., 1974. *Image Science,* (Academic Press: London).

Furenlid, I., Schoening, W.E. & Carder, B.E., 1977. *AAS Photo-Bulletin,* **16**, 14.

Hawkins, M.R.S., 1991. IAU Working Group on Wide Field Imaging, Newsletter No. 1, p. 23.

Heydon-Dumbleton, N.H., Collins, C.A. & MacGillivray, H.T., 1989. *Mon. Not. R. astron. Soc.*, **238**, 379.

Irwin, M.J., 1992. In "*Digitised Optical Sky Surveys*", eds. H.T. MacGillivray and E.B. Thomson. (Kluwer: Holland), p. 43.

Malin, D.F., 1988. In "*Astrophotography, Proc. IAU*". (Springer: Berlin), p. 125.

Marriage, A. & Pitts, E., 1956. *J. Opt. Soc. Am.*, **46**, 1019.

Shopbell, P.L., Bland-Hawthorn, J. & Malin, D.F., 1992. *Astron. J.*, in press.

Trabka, E.A., 1969. *J. Opt. Soc. Am.*, **59**, 662.

Tsvetkov, M.K., 1992. IAU Working Group on Wide-Field Imaging, Newsletter No. 2, p. 51.

West, R.M., 1991. *ESO Messenger,* **65**, 45.

Jonathan Bland-Hawthorn and Patrick L. Shopbell
Dept. of Space Physics and Astronomy
Rice University
Houston
TX 77251
U.S.A.